Latest cosmological constraints on the densities of hot and cold dark matter

Max Tegmark[1], Matias Zaldarriaga[2], and Andrew J. S. Hamilton[3]

[1] Dept. of Physics, Univ. of Pennsylvania, Philadelphia, PA 19104; max@physics.upenn.edu
[2] Institute for Advanced Study, Princeton, NJ 08540; matiasz@ias.edu
[3] JILA and Astrophysical and Planetary Sciences, Box 440, Univ. of Colorado, Boulder, CO 80309; Andrew.Hamilton@colorado.edu

Abstract. As experimentalists step up their pursuit of cold dark matter particles and neutrino masses, cosmological constraints are tightening. We compute the joint constraints on 11 cosmological parameters from cosmic microwave background and large scale structure data, and find that at 95% confidence, the total (cold+hot) dark matter density is $h^2\Omega_{\rm dm} = 0.20^{+.12}_{-.10}$ with at most 38% of it being hot (due to neutrinos). A few assumptions, including negligible neutrinos, tighten this measurement to $h^2\Omega_{\rm dm} = 0.13^{+0.04}_{-0.02}$, *i.e.*, 2.4×10^{-27}kg/m^3 give or take 20%.

1 INTRODUCTION

The cosmic microwave background (CMB) is dramatically improving our knowledge of cosmological parameters [1,2,3,4,5,6,7]. However, since the CMB still suffers from so-called degeneracies, where the effect of changing some parameters can be almost canceled by changing others, even more information can be extracted if additional information is included in the analysis. The power spectrum of large scale structure (LSS) in the galaxy distribution is particularly powerful in this regard, since it is depends on almost all of the parameters that affect the CMB, but in different ways since the physics involved is different. Since the sources of systematic errors are also different, a joint CMB+LSS analysis has the additional merit of allowing a number of consistency checks to be made.

In this paper, we will perform such a joint CMB+LSS analysis using the data shown in Figure 1. We include all currently available CMB data [8]. The LSS data is the linear real space power spectrum of the *IRAS* Point Source Catalogue Redshift Survey [9] (PSCz) as measured by [10]. The PSCz survey contains 18,351 galaxies covering 84% of the sky to a usable depth of about $400\,h^{-1}$Mpc. Earlier CMB+LSS work [11,12,13,14,15,16,17,18,19,20,21] was recently extended using LSS-information summarized by two parameters [1,6] — here we treat the LSS data just as the CMB, including the full power spectrum shape.

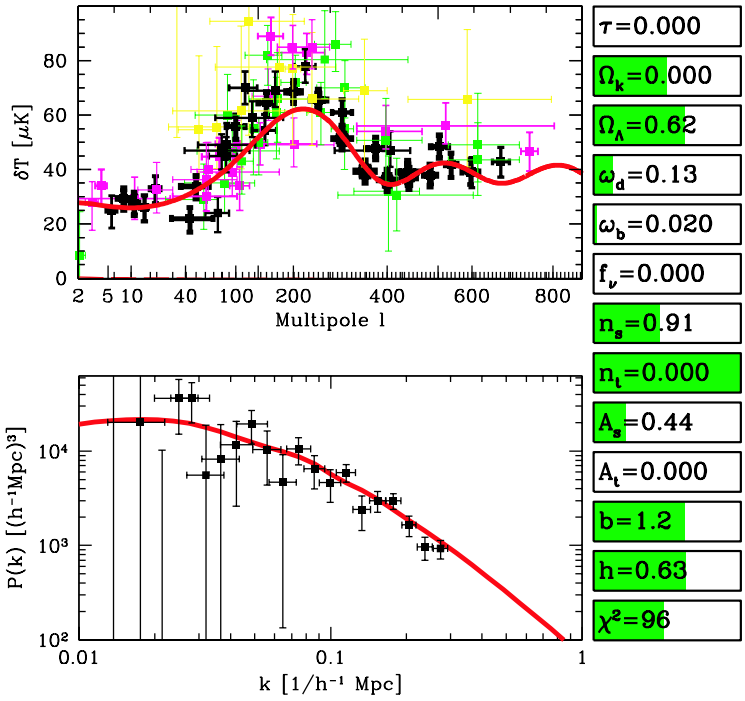

Fig. 1. The data used is shown for the CMB (top) and the LSS (bottom) together with the best fit "concordance" model from Table 1. Animated versions of this figure, where the effect of changing one parameter at a time can be viewed, are available at www.hep.upenn.edu/∼max/concordance.html.

2 METHOD

Our goal is to constrain jointly the 11 cosmological parameters

$$\mathbf{p} \equiv (\tau, \Omega_{\rm k}, \Omega_\Lambda, \omega_{\rm dm}, \omega_{\rm b}, f_\nu, n_s, n_t, A_s, A_t, b). \quad (1)$$

These are the reionization optical depth τ, the primordial amplitudes A_s, A_t and tilts n_s, n_t of scalar and tensor fluctuations, a bias parameter b defined as the ratio between rms galaxy fluctuations and rms matter fluctuations on large scales, and five parameters specifying the cosmic matter budget. The various contributions Ω_i to critical density are for curvature $\Omega_{\rm k}$, vacuum energy Ω_Λ, cold dark matter $\Omega_{\rm cdm}$, hot dark matter (neutrinos) Ω_ν and baryons $\Omega_{\rm b}$. The quantities $\omega_{\rm b} \equiv h^2\Omega_{\rm b}$ and $\omega_{\rm dm} \equiv h^2\Omega_{\rm dm}$ correspond to the physical densities of baryons and total (cold + hot) dark matter ($\Omega_{\rm dm} \equiv \Omega_{\rm cdm} + \Omega_\nu$), and $f_\nu \equiv \Omega_\nu/\Omega_{\rm dm}$ is the fraction of the dark matter that is hot. We assume that the bias b is constant on large scales but make no assumptions about its value, and therefore marginalize over this parameter before quoting constraints on the other ten.

Just as in particle physics, it is possible to extend this "minimal standard model" by introducing more physics and more parameters. We limit our analysis to these 11 since they are all so well-motivated theoretically or observationally that it would be inappropriate to leave them out or to assume that we know their values *a priori*.

Our method consists of the following steps:

1. Compute power spectra C_ℓ and $P(k)$ for a grid of models in our 11-dimensional parameter space.
2. Compute a likelihood for each model that quantifies how well it fits the data.
3. Perform 11-dimensional interpolation and marginalize to obtain constraints on individual parameters and parameter pairs.

To make step 1 feasible in practice, we recently developed a method for accelerated power spectrum calculation [22] that speeds up the widely used CMBfast software [23] by a factor around 10^3 without appreciable loss of accuracy. The details of our calculations and assumptions are given in the above-mentioned paper — the results below summarize the parts of the conclusions of greatest interest to a particle physics audience.

3 RESULTS

3.1 Basic results

Our constraints on individual cosmological parameters are listed in Table 1 for three cases and plotted in Figure 2 for them. All tabulated and plotted bounds are 95% confidence limits. The first case uses constraints from CMB alone, which are still rather weak because of degeneracy problems. The second case combines the CMB information with the power spectrum measurements from PSCz, and is seen to give rather interesting constraints on most parameters except the tensor tilt n_t. The third case adds three assumptions: that the latest measurements of the baryon density $\omega_{\rm b} = 0.019 \pm 0.0024$ from Big Bang Nucleosynthesis (BBN) are correct [24], that the 1σ constraints on the Hubble parameter are $h = 0.74 \pm 0.08$ [25], and that the neutrino contribution is cosmologically negligible. The neutrino assumption is that there is no strong mass-degeneracy between the relevant neutrino families, and that the Super-Kamiokande atmospheric neutrino data therefore sets the scale of the neutrino density to be $\omega_\nu \sim \times 10^{-4} - 10^{-3}$ [26]. We emphasize that this last assumption (that the heaviest neutrino weighs of order the root of the squared mass difference $\Delta m^2 \sim 0.07{\rm eV}^2$) is merely motivated by Occam's razor, not by observational evidence — the best current limits on f_ν from other astrophysical observations (see [27] and references therein) are still compatible with $f_\nu \sim 0.2$. Rather, we have chosen to highlight the consequences of this prior since, as discussed below, it has interesting effects on other parameters.

Table 1 – Best fit values and 95% confidence limits on cosmological parameters. The "concordance" case combines CMB and PSCz information with a BBN prior $\omega_{\rm b} = 0.02$, a Hubble prior $h = 0.74 \pm 0.08$ and a prior that $f_\nu \sim 10^{-3}$. A dash indicates that no meaningful constraint was obtained. The redshift space distortion parameter is $\beta \equiv f(\Omega_{\rm m}, \Omega_\Lambda)/b$, where f is the linear growth rate. z_{ion} is the redshift of reionization and t_0 is the present age of the Universe in Gigayears.

	CMB alone			CMB + PSCz			Concordance		
Quantity	Min	Best	Max	Min	Best	Max	Min	Best	Max
τ	0.0	0.0	0.32	0.0	0.0	.44	0.0	0.0	.16
$\Omega_{\rm k}$	$-.69$	$-.34$	0.05	$-.19$	$-.02$	0.10	$-.05$	$-.00$	0.08
Ω_Λ	.05	.43	.92	–	.38	0.76	.49	.62	0.74
$h^2\Omega_{\rm dm}$	0.0	.10	–	.10	.20	0.32	.11	.13	0.17
$h^2\Omega_{\rm b}$	.024	.054	.103	.020	.028	.037	*.02*	*.02*	*.02*
f_ν	0.0	.80	1.0	0.0	.22	.38	$\sim$*0*	$\sim$*0*	$\sim$*0*
n_s	.91	1.43	–	0.86	.96	1.16	0.84	.92	1.01
n_t	–	0.0	–	–	0.0	–	–	0.0	–
b	–	–	–	.75	1.26	1.78	.87	1.10	1.33
h	.18	.53	.88	.33	.59	.86	.58	.68	.78
β	–	–	–	.37	.63	.89	.36	.51	.66
z_{ion}	0	7	21	0	9	26	0	6	20
t_0	8.4	15.6	23.0	9.6	13.3	17.0	12.1	13.4	14.6

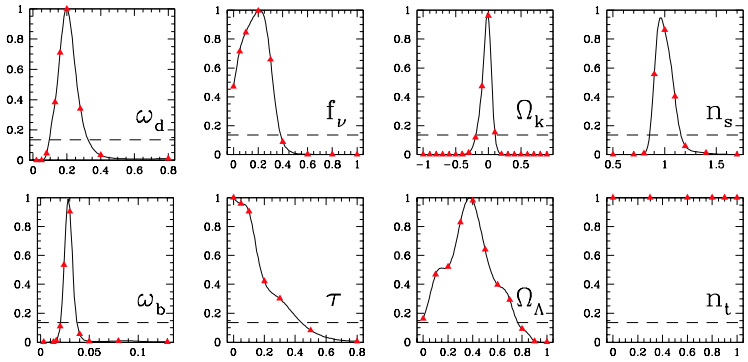

Fig. 2. Constraints on individual parameters using only CMB and LSS information. The quoted 95% confidence limits are where each curve drops below the dashed line.

3.2 Effects of priors

The joint CMB+PSZc constraints are remarkably robust to prior assumptions. Imposing priors such as flatness ($\Omega_{\rm k} = 0$), no tensors ($r = 0$), no tilt ($n_s = 1$), no reionization ($\tau = 0$), and a reasonable Hubble parameter (we tried both $h = 0.74 \pm 8$ at 65% and the weaker constraint $50 < h < 100$ at 95%), both alone and in various combinations, has little effect. The fact that the best fit

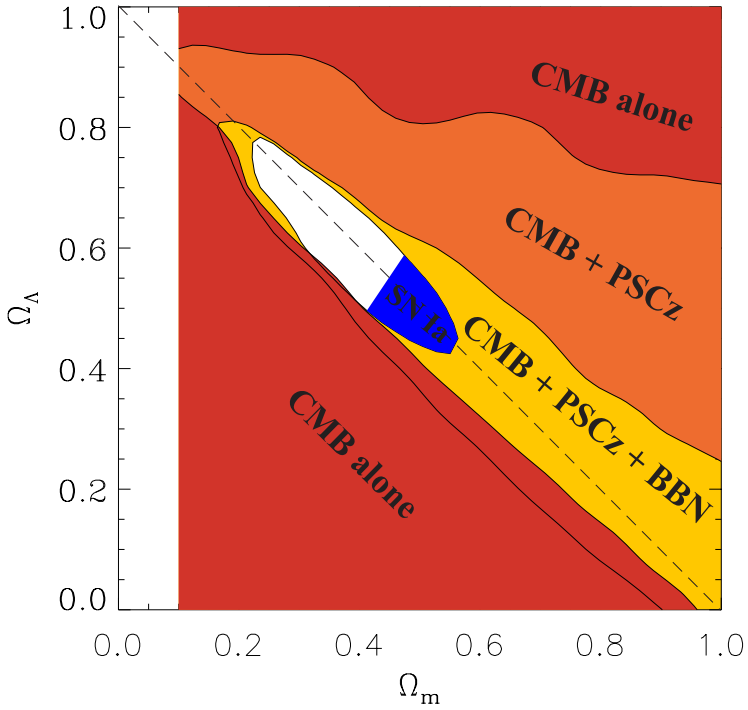

Fig. 3. Constraints in the $(\Omega_{\rm m}, \Omega_\Lambda)$-plane. The shaded regions are ruled out at 95% confidence by the information indicated. The allowed (white) region is seen to be centered around flat models, which fall on the dashed line.

parameter values are not appreciably altered reflects that these priors all agree well with what is already borne out by the CMB+PSCz data: $\Omega_{\rm k} \sim r \sim \tau \sim 0$, and $n_s \sim 1$. The fact that these priors do not shrink the error bars much on other parameters indicates that PSCz has already broken the main CMB degeneracies.

The nucleosynthesis prior has a greater influence because it does not agree all that well with what the CMB+LSS data prefer. We found one additional prior that had a non-negligible effect: that on neutrinos. As illustrated in Figure 6, inclusion of neutrinos substantially weakens the upper limits on the dark matter density. Since the neutrino fraction f_ν has only a weak effect on the CMB, this effect clearly comes from LSS. A larger dark matter density $\omega_{\rm dm}$ pushes matter-radiation equality back to an earlier time, shifting the corresponding turnover in $P(k)$ to the right and thereby increasing the ratio of small-scale to large-scale power. Increasing the neutrino fraction counteracts this by suppressing the small-scale power (without affecting the CMB much), thereby weakening the upper limit on $\omega_{\rm dm}$. Imposing the prior $f_\nu = 0$ alone, without nucleosynthesis or Hubble priors, tightens the CMB+PSCz constraint $\omega_{\rm dm} < 0.32$ from Table 1 to $\omega_{\rm dm} < 0.19$.

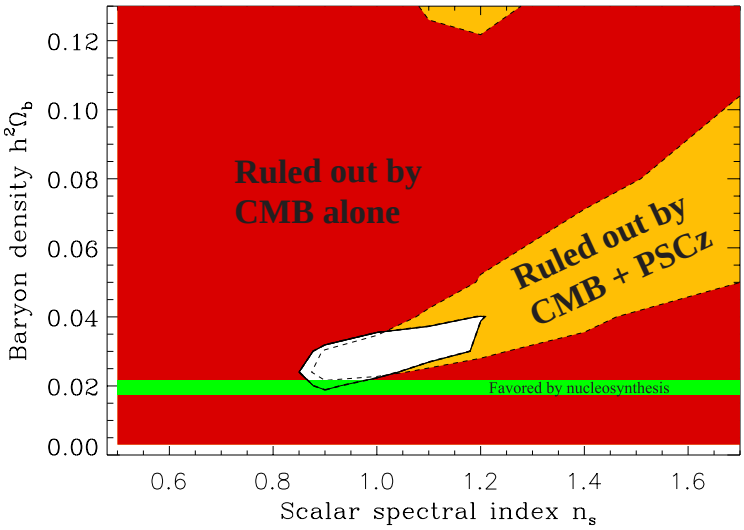

Fig. 4. Constraints in the (n_s, ω_b)-plane. Note that PSCz not only shrinks the allowed region (white), but also pushes it slightly down to the left (the dashed line indicates the CMB-only boundary).

4 DISCUSSION

We have presented joint constraints on 11 cosmological parameters from current CMB and galaxy clustering data. Perhaps the most interesting results of this paper are the numbers themselves, listed in the CMB+LSS columns of Table 1, and their striking robustness to imposing various priors. A superficial glance at the constraint figures might suggest that little has changed since the first analysis of Boomerang + Maxima [2], or even since the pre-Boomerang analysis of [28], since the plots look rather similar. However, whereas these earlier papers obtained strong constraints only with various poorly justified priors such as no tensors, no tilt or no curvature, the joint CMB + LSS data are now powerful enough to speak for themselves, without needing any such prior props.

4.1 Towards a refined concordance model

It is well-known that different types of measurements can complement each other by breaking degeneracies. However, even more importantly, multiple data sets allow numerous consistency checks to be made. The present results allow a number of such tests.

Baryons Perhaps the most obvious one involves the baryon fraction. Although there is still some tension between BBN (preferring $\omega_b \sim 0.02$) and CMB+LSS (preferring $\omega_b \sim 0.03$), an issue which will undoubtedly be clarified by improved

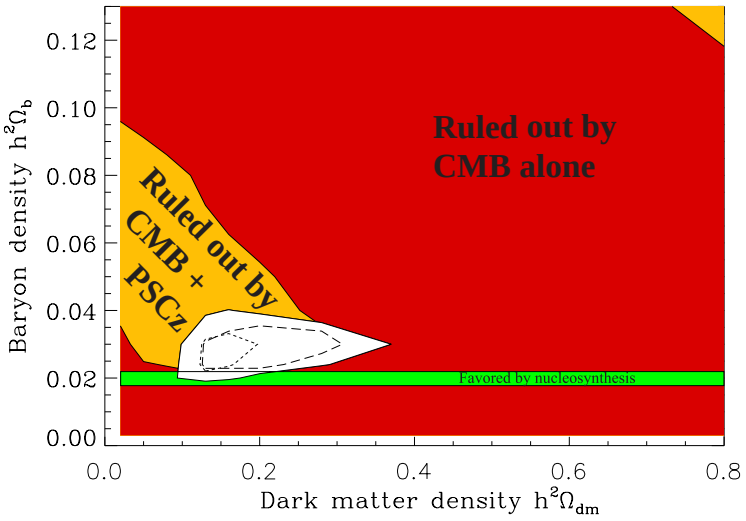

Fig. 5. Constraints in the $(\omega_{\rm dm}, \omega_{\rm b})$-plane. As in the previous figure, adding PSCz prohibits high baryon solutions and allows slightly lower $\omega_{\rm b}$-values than CMB alone. The dashed curve within the allowed (white) region show the sharper constraint obtained when imposing the priors for a flat, scalar scale-invariant model ($\Omega_{\rm k} = r = 0$, $n_s = 1$). The dotted curve shows the effect of requiring negligible neutrino density ($f_\nu \sim 0$) in addition.

data within a year, the most striking point is that the methods agree as well as they do. That one method involving nuclear physics when the Universe was a minute old and another involving plasma physics more than 100,000 years later give roughly consistent answers, despite involving completely different systematics, can hardly be described as anything short of a triumph for the Big Bang model.

It is noteworthy that our addition of LSS information pulls down the baryon value slightly, so that a BBN-compatible value $\omega_{\rm b} = 0.02$ is now within the 95% confidence interval. Part of the reason that that the CMB alone gave a stronger lower limit may be a reflection of the Bayesian likelihood procedure employed in this and all other recent papers on the topic: when a large space of high $\omega_{\rm b}$-values are allowed, the relative likelihood for lower values drops.

Dark energy Another important cross-check involves the cosmological constant. Although the constraint $0.49 < \Omega_\Lambda < 0.74$ from Table 1 does not involve any supernova information, it agrees nicely with the recent accelerating universe predictions from SN 1a [29,30]. This agreement is illustrated in Figure 3, which shows the SN 1a constraints from [31] combining the data from both teams. As frequently pointed out, the conclusion $\Omega_{\rm m} \sim 0.35$ also agrees well with a number

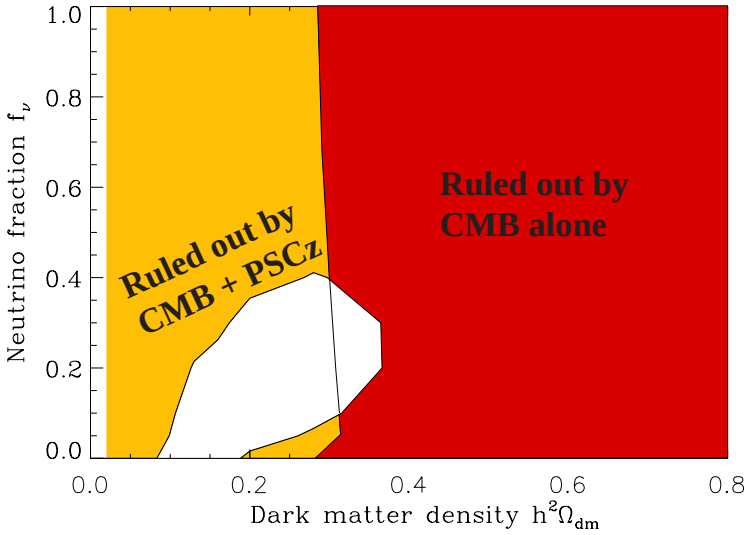

Fig. 6. Constraints in the $(\omega_{\rm dm}, f_\nu)$-plane. The shape of the allowed (white) region explains why the prior $f_\nu = 0$ tightens the upper limit on the dark matter density. The vertical line shows the CMB-only boundary before PSCz is added.

of other observations, *e.g.*, the cluster abundance at various redshifts and cosmic velocity fields.

Bias A third cross-check is more subtle but equally striking, involving the bias of the PSCz galaxies — we can measure it in two completely independent ways. One is by comparing the amplitude of the CMB and galaxy power spectra, which gives the constraints listed in Table 1. The other way is via linear redshift space distortions. In terms of the redshift space distortion parameter $\beta \approx \Omega_{\rm m}^{0.6}/b$, the former method gives $\beta = 0.51 \pm 0.08$ and the latter gives $\beta = 0.45^{+.14}_{-.12}$ (68%). This striking agreement means that a highly non-trivial consistency test has been passed.

4.2 Concordance

In conclusion, the simple "concordance" model in the last columns of Table 1 (plotted in Figure 1) is at least marginally consistent with all basic cosmological constraints, including CMB, PSCz and nucleosynthesis. Specifically, as discussed above, our calculations show that it has passed three non-trivial consistency tests. Moreover our concordance model is encouragingly robust towards imposing a score of prior constraints in various combinations. In summary, the non-baryonic matter that is the topic of this conference really seems to be out there, and we now have quite strong indications of what its mean density is: $2.4 \times 10^{-27}{\rm kg/m}^3$ give or take 20%.

The authors wish to thank Angélica de Oliveira-Costa, Brad Gibson, Wayne Hu and Nikhil Padmanabhan for useful discussions. Support for this work was provided by NSF grant AST00-71213, NASA grants NAG5-7128 and NAG5-9194, the University of Pennsylvania Research Foundation, and Hubble Fellowship HF-01116.01-98A from STScI, operated by AURA, Inc. under NASA contract NAS5-26555.

References

1. A. E. Lange *et al.*: astro-ph/0005004 (2000).
2. M. Tegmark and M. Zaldarriaga: astro-ph/0004393 (2000).
3. A. Balbi *et al.*: astro-ph/0005124 (2000).
4. S. L. Bridle *et al.*: astro-ph/0006170 (2000).
5. W. Hu, M. Fukugita, M. Zaldarriaga, and M. Tegmark: astro-ph/0006436 (2000).
6. A. Jaffe *et al.*: astro-ph/0007333 (2000).
7. W. Kinney, A. Melchiorri, and A. Riotto: astro-ph/0007375 (2000).
8. E. Gawiser and J. Silk: astro-ph/0002044 (2000).
9. W. Saunders *et al.*: astro-ph/0001117 (2000).
10. A. J. S Hamilton, M. Tegmark, and N. Padmanabhan: astro-ph/0004334 (2000).
11. G. Efstathiou, J. R. Bond, and S. D. M White: MNRAS **258**, 1 (1992).
12. L. A. Kofman, N. Y. Gnedin, and N. A. Bahcall: ApJ **413**, 1 (1993).
13. M. White, Pedro. P. T Viana P, A. R. Liddle, and D. Scott: MNRAS **283**, 107 (1996).
14. A. R. Liddle, D. H. Lyth, T. P. T Viana, and M. White: MNRAS **282**, 281L (1996).
15. E. F. Bunn and M. White: ApJ **480**, 6 (1997).
16. E. Gawiser and J. Silk: Science **280**, 1405 (1998).
17. M. Webster *et al.*: ApJL **509**, L65 (1998).
18. J. R. Bond and A. H. Jaffe: astro-ph/9809043 (1998).
19. N. Bahcall, J. P. Ostriker, S. Perlmutter,, and P. J. Steinhardt: Science **284**, 1481 (1999).
20. B. Novosyadlyj, R. Durrer, S. Gottlb̈er, V. N. Lukash, and S. Apunevych: A&A **356**, 418 (2000).
21. S. L. Bridle, V. L. Eke, O. Lahav, A. N. Lasenby, M. P. Hobson, S. Cole, C. S. Frenk, and J. P. Henry: MNRAS **310**, 565 (1999).
22. M. Tegmark, M. Zaldarriaga, and A. J. S Hamilton: astro-ph/0008167 (2000).
23. U. Seljak and M. Zaldarriaga: ApJ **469**, 437 (1996).
    M. Zaldarriaga and U. Seljak: astro-ph/9911219 (1999).
24. S. Burles, K. M. Nollett, J. N. Truran, and M. S. Turner: astro-ph/9901157 (1999).
25. W. Freedman *et al.* 2000, in preparation
26. K. Scholberg *et al.*: hep-ex/9905016 (1999).
27. R. A. C Croft, W. Hu, and R. Davé: Phys. Rev. Lett. **83**, 1092 (1999).
28. M. Tegmark and M. Zaldarriaga: astro-ph/0002091 (2000).
29. S. Perlmutter *et al.*: Nature **391**, 51 (1998).
30. A. G. Riess *et al.*: Astron. J. **116**, 1009 (1998).
31. M. White: ApJ **506**, 495 (1998).